

Shift spin photocurrents in two-dimensional systems

Hsiu-Chuan Hsu^{1,2,*} and Tsung-Wei Chen^{3,†}

¹*Graduate Institute of Applied Physics, National Chengchi University, Taipei 11605, Taiwan*

²*Department of Computer Science, National Chengchi University, Taipei 11605, Taiwan*

³*Department of Physics, National Sun Yat-sen University, Kaohsiung 80424, Taiwan*

(Dated: March 13, 2025)

The generation of nonlinear spin photocurrents by circularly polarized light in two-dimensional systems is theoretically investigated by calculating the shift spin conductivities. In time-reversal symmetric systems, shift spin photocurrent can be generated under the irradiation of circularly polarized light, while the shift charge photocurrent is forbidden by symmetry. We show that the k -cubic Rashba-Dresselhaus system, the k -cubic wurtzite system and Dirac surface states can support the shift spin photocurrent. By symmetry analysis, it is found that in the Rashba type spin-orbit coupled systems, mirror symmetry requires that the spin polarization and the moving direction of the spin photocurrent be parallel, which we name longitudinal shift spin photocurrent. The Dirac surface states with warping term exhibit mirror symmetry, similar to the Rashba type system, and support longitudinal shift spin photocurrent. In contrast, in the Dresselhaus type spin-orbit coupled systems, the parity-mirror symmetry requires that the spin polarization and the moving direction of the spin photocurrent be perpendicular, which we dub transverse shift spin photocurrent. Furthermore, we find that the shift spin photocurrent always vanishes in any k -linear spin-orbit coupled system unless the Zeeman coupling μ_z is turned on. We find that the splitting of degenerate energy bands due to Zeeman coupling μ_z causes the van Hove singularity. The resulting shift spin conductivity has a significant peak at optical frequency $\omega = 2\mu_z/\hbar$.

I. INTRODUCTION

The bulk photovoltaic effect is the generation of DC current under the irradiation of light without applied bias; thus, its role in green energy applications has been actively investigated [1–4]. Moreover, the bias-free mechanism allows a noninvasive device fabrication of charge injection that reduces defects, leading to enhanced device quality [5]. Recent studies have demonstrated that the bulk photovoltaic effect is closely related to the geometrical properties of Bloch states [6–8], stretching the fundamental understanding of materials beyond energy bands [9]. The bulk photovoltaic effect has been shown to originate from the Berry curvature [10], quantum metric [11] and Christoffel symbols [7, 12].

The requirement for the bulk photovoltaic effects is the breaking of inversion symmetry [13]. Low-dimensional systems naturally lack the inversion symmetry and could support bulk photovoltaic effect [2, 14]. Typical examples include the two-dimensional electron gas in a semiconductor heterostructure and boundary modes of a bulk material. Furthermore, two types of spin-orbit coupling are often present in two-dimensional systems: Rashba spin-orbit coupling, which arises from broken structural inversion symmetry and can be induced by a built-in electric field, and Dresselhaus spin-orbit coupling, which results from inversion asymmetry in the bulk lattice [14, 15]. The bulk photovoltaic effect is a second-order optical response and includes two types of mechanism: injection and shift photocurrents [16, 17].¹ The injection photocurrent is linearly proportional to the charge relaxation time,

while the shift photocurrent is independent of the charge relaxation time. The shift photocurrent is described by the interband Berry connections of Bloch states and can be understood as the shift of wave packet upon interband transitions [1, 2]. In time-reversal symmetric systems, the shift charge currents can be generated by linearly polarized light, but not by circularly polarized light [7, 17].

In addition to the bulk photovoltaic effect for electron charges, the bulk photovoltaic effect for spins has attracted much attention [5, 19, 20] for its potential application in spintronics. It has been shown that spin photocurrent can be driven by the same mechanisms as the bulk photovoltaic effect, as derived by second-order response theory [5, 19, 21]. Similar to the shift charge current, the shift spin photocurrent is related to the Berry connections, in addition to the spin current operator. Due to the different selection rules for charge and spin, it has been shown that under certain symmetry constraints, it is possible to generate pure spin current without any charge current. Recently, pure spin photocurrent generation has been studied in altermagnetic insulators [22, 23]. The detailed symmetry analysis shows that when the altermagnetic insulators are irradiated by circularly polarized light, the shift spin photocurrent is zero in the absence of spin-orbit coupling, whereas the injection spin photocurrent can be nonzero regardless of spin-orbit coupling [22].

In time-reversal symmetric systems, the shift spin photocurrent can be generated under the circularly polarized light, while the shift charge current is forbidden. However, the shift spin photocurrents under circularly polarized light have been overlooked until recently [5, 21]. Motivated by this issue, in this paper, we theoretically study the shift spin photocurrents generated by circularly polarized light in perfect two-dimensional systems with spin-orbit interactions. In the absence of Zeeman coupling, we show that the shift spin photocurrents can be generated only in some higher- k systems (Wurtzite, k -cubic Dresselhaus and k -cubic Rashba-

* hcjhsu@nccu.edu.tw

† twchen@mail.nsysu.edu.tw

¹ In addition to current, the static magnetization can be generated by light in the second-order response, referred to as the nonlinear Edelstein effect [18].

Dresselhaus systems) and Dirac surface states with preserved time-reversal symmetry. In the k -linear systems, the shift spin photocurrent can only be generated in the presence of the Zeeman coupling. We also discuss how mirror symmetry constrains the nonzero components of the shift spin conductivity tensors. The remainder of this paper is as follows. In Sec. II and Sec. III, the general two-band Hamiltonian and the shift spin conductivity are introduced, respectively. The results are given in the following sections. In Sec. IV, the symmetry analysis is given. In Sec. V, the results for systems with isotropic dispersions are given. In Sec. VI, the results for systems with non-isotropic dispersions are presented. Lastly, a conclusion is given in Sec. VII.

II. EFFECTIVE HAMILTONIAN

The generic spin-orbit coupled Hamiltonian H_0 for the system with two energy bands can be written as

$$H_0 = \epsilon_{\mathbf{k}} + \sigma_x d_x(\mathbf{k}) + \sigma_y d_y(\mathbf{k}) + \sigma_z d_z(\mathbf{k}), \quad (1)$$

where $\epsilon_k = \hbar^2 k^2 / 2m$ is the kinetic energy, and σ_x, σ_y and σ_z are Pauli matrices representing spins of the charged particles. We only consider two-dimensional systems, the momentum \mathbf{k} has no k_z component, i.e., $\mathbf{k} = (k_x, k_y)$. When an external magnetic field B is applied along the z -axis, the Zeeman coupling is given by $\frac{1}{2}g\mu_B\sigma_z B$, where g and μ_B represent g -factor and Bohr magneton, respectively. This coupling introduces an additional term to $d_z(\mathbf{k})$ in Eq. (1). In the following discussion, we define the Zeeman coupling as $\mu_z = \frac{1}{2}g\mu_B B$.

We choose the eigenvectors of Eq. (1) as

$$\begin{aligned} |+\mathbf{k}\rangle &= \frac{1}{\sqrt{2(1+\hat{d}_z)}} \begin{pmatrix} -\hat{d}_x + i\hat{d}_y \\ 1 + \hat{d}_z \end{pmatrix}, \\ |-\mathbf{k}\rangle &= \frac{1}{\sqrt{2(1+\hat{d}_z)}} \begin{pmatrix} 1 + \hat{d}_z \\ \hat{d}_x + i\hat{d}_y \end{pmatrix}, \end{aligned} \quad (2)$$

where $d = \sqrt{d_x^2 + d_y^2 + d_z^2}$ and $\hat{d}_x = d_x/d$, and so on. It is easy to show that Eq. (2) satisfies the orthonormal property and completeness, i.e.,

$$\sum_{n=\pm 1} |n\mathbf{k}\rangle \langle n\mathbf{k}| = 1, \quad \langle n\mathbf{k}|m\mathbf{k}\rangle = \delta_{nm}. \quad (3)$$

The corresponding eigen-energy is given by

$$H_0|n\mathbf{k}\rangle = E_{n\mathbf{k}}|n\mathbf{k}\rangle, \quad n = \pm 1 \quad (4)$$

with

$$E_{n\mathbf{k}} = \epsilon_{\mathbf{k}} - nd(\mathbf{k}). \quad (5)$$

We note that the band index $n = +1$ corresponds to the lower energy $E_{+\mathbf{k}} = \epsilon_{\mathbf{k}} - d$ and $n = -1$ corresponds to the higher energy $E_{-\mathbf{k}} = \epsilon_{\mathbf{k}} + d$. The diagonal and off-diagonal matrix elements of spin operator in the basis Eq. (2) are given in Appendix B 1.

k -linear system	(d_x, d_y, d_z)	d
Generic	$(\beta_{xx}k_x + \beta_{xy}k_y, \beta_{yx}k_x + \beta_{yy}k_y, 0)$	$d = k\Gamma_1(\phi)$
Rashba	$\alpha_0(k_y, -k_x, 0)$	$d = \alpha_0 k$
Dresselhaus	$\beta_0(-k_x, k_y, 0)$	$d = \beta_0 k$
Rash.-Dress.	$(-\beta_0 k_x + \alpha_0 k_y, -\alpha_0 k_x + \beta_0 k_y, 0)$	$d = k\Gamma_2(\phi)$
Weyl	$\eta(k_x, k_y, 0)$	$d = \eta k$
PST	$\lambda(k_x - k_y, k_x - k_y, 0)$	$d = k\Gamma_3(\phi)$

TABLE I. Five spin-orbit coupled systems with linear momentum in k .

k -cubic system	(d_x, d_y, d_z)	d
Rashba	$\alpha(k_y(3k_x^2 - k_y^2), k_x(3k_y^2 - k_x^2), 0)$	$d = \alpha k^3$
Dresselhaus	$-\beta k^2(k_x, k_y)$	$d = \beta k^3$
Rash.-Dress.	$(\alpha k_y(3k_x^2 - k_y^2) - \beta k^2 k_x, \alpha k_x(3k_y^2 - k_x^2) - \beta k^2 k_y, 0)$	$d = k^3\Gamma_2(\phi)$
Wurtzite	$(\alpha' + \beta' k^2)(k_y, -k_x, 0)$	$d = \alpha' k + \beta' k^3$

TABLE II. Four spin-orbit coupled systems with k^3 .

For typical spin-orbit coupled systems linearly in momentum k are shown in Table I, including Rashba [24–27], Dresselhaus [28–31], Rashba-Dresselhaus, Weyl [32, 33], persistent-spin-texture (PST) [34] and generic systems [35–37]. The PST system is a special case of linear Rashba-Dresselhaus system when $\beta_0 = \alpha_0$. In Table I, the functions $\Gamma_1(\phi)$, $\Gamma_2(\phi)$ and $\Gamma_3(\phi)$ are given by

$$\begin{aligned} \Gamma_1(\phi)^2 &= (\beta_{xx}^2 + \beta_{yy}^2) \cos^2 \phi + (\beta_{xy}^2 + \beta_{yx}^2) \sin^2 \phi \\ &\quad + (\beta_{xx}\beta_{xy} + \beta_{yx}\beta_{yy}) \sin(2\phi) \end{aligned} \quad (6)$$

and

$$\begin{aligned} \Gamma_2(\phi) &= \sqrt{\alpha_0^2 + \beta_0^2 - 2\alpha_0\beta_0 \sin(2\phi)}, \\ \Gamma_3(\phi) &= \sqrt{2\lambda\sqrt{1 - \sin(2\phi)}}. \end{aligned} \quad (7)$$

The azimuthal angle ϕ is defined as $\tan \phi = k_y/k_x$.

Typical k -cubic systems are shown in Table II, including Rashba [38, 39], Dresselhaus [40], Rashba-Dresselhaus [41], and Wurtzite [42, 43] systems. In Table II, the functions $\Gamma_2(\phi)$ for k -cubic Rashba-Dresselhaus system is the first line of Eq. (7) by the replacement $\alpha_0 \rightarrow \alpha$ and $\beta_0 \rightarrow \beta$.

III. SHIFT SPIN CONDUCTIVITY

In this section, we calculate the shift spin conductivity for the system Hamiltonian Eq. (1). The shift spin (charge) conductivity is written as [21]

$$\sigma^{Ic;ab} = \frac{-i\pi e^3}{\hbar^2} \int_{\mathbf{k}} \sum_{nm} (f_n - f_m) M_{mn}^{Ic;ab} \delta(\omega_{mn} - \omega), \quad (8)$$

where f_n represents Fermi-Dirac distribution and $\omega_{mn} = (E_m - E_n)/\hbar$. The superscript $I = 0$ represents the shift

charge current and $I = x, y, z$ means spin polarization. We focus on the shift spin photocurrent induced by the circular light ($a = x, b = y$), and thus, we consider the imaginary part of Eq. (8),

$$\text{Im}[\sigma^{Ic;ab}] = \frac{-\pi e^3}{\hbar^2} \int_{\mathbf{k}} \sum_{nm} (f_n - f_m) \text{Re}[M_{mn}^{Ic;ab}] \delta(\omega_{mn} - \omega). \quad (9)$$

The matrix element $M_{mn}^{Ic;ab}$ is given by

$$M_{mn}^{Ic;ab} = \frac{v_{nm}^b}{\omega_{mn}^2} K_{mn}^{ca} - \frac{v_{mn}^a}{\omega_{nm}^2} K_{nm}^{cb}, \quad (10)$$

where K_{mn}^{ca} and K_{nm}^{cb} are given by

$$\begin{aligned} K_{mn}^{ca} &= d_{mn}^{ca} - L_{mn}^{ca}, \\ K_{nm}^{cb} &= d_{nm}^{cb} - L_{nm}^{cb}, \end{aligned} \quad (11)$$

and matrix element d_{mn}^{ca} is

$$\begin{aligned} d_{mn}^{ca} &= J_{mn}^{Ica} + \sum_{p \neq m, n} \left(\frac{J_{mp}^{Ic} v_{pn}^a}{\omega_{mp}} - \frac{v_{mp}^a J_{pn}^{Ic}}{\omega_{pn}} \right), \\ d_{nm}^{cb} &= J_{nm}^{Icb} + \sum_{p \neq m, n} \left(\frac{J_{np}^{Ic} v_{pm}^b}{\omega_{np}} - \frac{v_{np}^b J_{pm}^{Ic}}{\omega_{pm}} \right), \end{aligned} \quad (12)$$

where

$$J^{Ica} = \frac{1}{2} \left\{ s_I, \frac{\partial^2 H_0}{\partial k_a \partial k_c} \right\}, \quad J^{Ic} = \frac{1}{2} \{ s_I, v^c \}, \quad (13)$$

and $s_I = \frac{1}{2} \sigma_I$ and σ_I stands for the Pauli matrix. The velocity operator v^c is given by $v^c = \frac{\partial(H_0/\hbar)}{\partial k_c}$. We note that the last term in the matrix element d_{mn}^{ca} is the virtual transition. The dummy index p in Eq. (12) stands for the summation over all bands except for the band indices m, n . The dominant contributions to the summation come from bands near the Fermi level within the photon energy [5, 44]. Thus, the error for effective Hamiltonians with finite number of bands is negligible in the low-frequency regime. A truncation-error-free scheme for shift charge current, particularly useful in *ab initio* calculations, has been developed in Ref. [45]. All the spin-orbit coupled systems considered in Table I and Table II describe spin-1/2 particles, except for the k -cubic Rashba and Dresselhaus Hamiltonians, which describe the heavy hole bands with total angular momentum 3/2 and the z components of $\pm 3/2$ [38, 39]. Thus, for k -cubic Hamiltonians s_I is replaced by $3s_I$. For convenience, the transport of the total angular momentum in cubic Hamiltonians is referred to as spin current, as used in the literature (e.g., [46, 47]) and discussed in App. A. On the other hand, the matrix element L_{mn}^{ca} is given by

$$\begin{aligned} L_{mn}^{ca} &= \frac{1}{\omega_{mn}} (J_{mn}^{Ic} \Delta_{mn}^a + v_{mn}^a \Delta_{mn}^{Ic}), \\ L_{nm}^{cb} &= \frac{1}{\omega_{nm}} (J_{nm}^{Ic} \Delta_{nm}^b + v_{nm}^b \Delta_{nm}^{Ic}), \end{aligned} \quad (14)$$

where $\Delta_{mn}^a = v_{mm}^a - v_{nn}^a$ and $\Delta_{mn}^{Ic} = J_{mm}^{Ic} - J_{nn}^{Ic}$. We note that $\omega_{mn}^2 = \omega_{nm}^2$ and Eq. (10) can be written as

$$\begin{aligned} M_{mn}^{Ic;ab} &= \frac{1}{\omega_{nm}^2} [(v_{nm}^b d_{mn}^{ca} - v_{mn}^a d_{nm}^{cb}) - (v_{nm}^b L_{mn}^{ca} - v_{mn}^a L_{nm}^{cb})] \\ &= \frac{1}{\omega_{nm}^2} (M_d - M_L), \end{aligned} \quad (15)$$

where M_d and M_L are defined as

$$\begin{aligned} M_d &= (v_{nm}^b d_{mn}^{ca} - v_{mn}^a d_{nm}^{cb}), \\ M_L &= (v_{nm}^b L_{mn}^{ca} - v_{mn}^a L_{nm}^{cb}). \end{aligned} \quad (16)$$

For the present case, we consider a two-band model [see Eq. (1)] and hence there is no virtual band transition. This implies that the matrix element d_{mn}^{ca} is given by

$$\begin{aligned} d_{mn}^{ca} &= J_{mn}^{Ica}, \\ d_{nm}^{cb} &= J_{nm}^{Icb}. \end{aligned} \quad (17)$$

Furthermore, the term Δ_{mn}^{Ic} will be exactly canceled in deriving $M^{Ic;ab}$, we can neglect it in the derivation. That is, we have

$$\begin{aligned} L_{mn}^{ca} &= \frac{1}{\omega_{mn}} J_{mn}^{Ic} \Delta_{mn}^a, \\ L_{nm}^{cb} &= \frac{1}{\omega_{nm}} J_{nm}^{Ic} \Delta_{nm}^b. \end{aligned} \quad (18)$$

Because $\omega > 0$, ω_{mn} in the Dirac-delta function must be positive. This implies that $m = -1$ and $n = +1$. After straightforward calculations, we have

$$M_d = v_{1,-1}^b J_{-1,1}^{Ica} - v_{-1,1}^a J_{1,-1}^{Icb} \quad (19)$$

and

$$M_L = \frac{1}{d} \left[v_{1,-1}^b J_{-1,1}^{Ic} \frac{\partial d}{\partial k_a} - v_{-1,1}^a J_{1,-1}^{Ic} \frac{\partial d}{\partial k_b} \right], \quad (20)$$

where we have used $E_{+\mathbf{k}} - E_{-\mathbf{k}} = -2d$ and $E_{-\mathbf{k}} - E_{+\mathbf{k}} = 2d$. The resulting matrix element $M_{mn}^{Ic;ab}$ is given by

$$M_{-1,1}^{Ic;ab} = \frac{\hbar^2}{4d^2} (M_d - M_L). \quad (21)$$

If we use the replacement $a \leftrightarrow b$, which means the change in the helicity of the circular polarized light, then by using Eqs. (19), (20) and (21), we have

$$\text{Re}[M_{-1,1}^{Ic;ba}] = -\text{Re}[M_{-1,1}^{Ic;ab}], \quad (22)$$

which only gives an overall sign. In the following calculations, we only calculate the six matrix elements of $\text{Re}[M_{-1,1}^{Ic;xy}]$, i.e., $I = x, y, z$ and $c = x, y$. The six matrix elements for the two-band model are given in Appendix B 2. For the two-dimensional cases, the spin lies on the two-dimensional plane and the spin z component only couples to the Zeeman interaction μ_z . Accounting for the case $d_z = \mu_z$, Eq. (B3) can be written as the following form. For in-plane spin $I = x, y$, we have

$$Re[M_{-1,1}^{Ic,xy}] = N \left\{ -sgn[\hat{e}_1] \frac{\mu_z^2}{d^2} \left[\frac{\partial d_I}{\partial k_{\hat{e}_1}} \left(1 - \frac{k_c}{d} \frac{\partial d}{\partial k_c} \right) + \frac{\partial d_I}{\partial k_c} \frac{k_c}{d} \frac{\partial d}{\partial k_{\hat{e}_1}} \right] + sgn[\hat{e}_2] G \frac{\hat{d}_{\hat{e}_2}}{d} k_c \left(1 - \frac{k}{d} \frac{\partial d}{\partial k} \right) \right\}. \quad (23)$$

For out-of-plane spin $I = z$ and $c = x, y$, we have

$$Re[M_{-1,1}^{zc,xy}] = N sgn[\hat{e}_1] \frac{\mu_z}{d} \frac{\partial d}{\partial k_{\hat{e}_1}}, \quad (24)$$

where we use the notation

$$\begin{aligned} \hat{e}_1 &= \hat{e}_c \times \hat{e}_z, \\ \hat{e}_2 &= \hat{e}_I \times \hat{e}_z, \end{aligned} \quad (25)$$

and we define $sgn[\hat{e}_x \times \hat{e}_z] = sgn[-\hat{e}_y] = -1$ and $sgn[\hat{e}_y \times \hat{e}_z] = sgn[+\hat{e}_x] = +1$. The term G and N are given in Eq. (B5), (B6) and (B8). The in-plane component Eq. (23) is composed of two terms, one is proportional to the square of Zeeman coupling μ_z^2 and the other term is independent of Zeeman coupling. The out-of-plane component Eq. (24) is linearly proportional to Zeeman coupling. When we turn off the Zeeman coupling, the out-of-plane component always vanishes, but the in-plane components may be non-zero. In the following sections, for the convenience of discussion, the matrix elements $Re[M_{-1,1}^{xx,xy}]$ and $Re[M_{-1,1}^{yy,xy}]$ (i.e., $I = c$) are called longitudinal components, and the matrix elements $Re[M_{-1,1}^{xy,xy}]$ and $Re[M_{-1,1}^{yx,xy}]$ (i.e., $I \neq c$) are called transverse components. The matrix elements $Re[M_{-1,1}^{zx,xy}]$ and $Re[M_{-1,1}^{zy,xy}]$ (i.e., $I = z$) are called out-of-plane components.

IV. SYMMETRY ANALYSIS

The two-dimensional systems studied in this work preserve mirror or parity-mirror symmetry. We discuss the symmetry constraints on shift spin conductivity imposed by the symmetry for the Rashba and Dresselhaus type Hamiltonians that commonly arise in two-dimensional systems. For simplicity, we take the k -linear Rashba and Dresselhaus spin-orbit coupling (SOC) as an example

$$h_R = \alpha_0(k_y \sigma_x - k_x \sigma_y), \quad (26)$$

$$h_D = \beta_0(k_x \sigma_x - k_y \sigma_y). \quad (27)$$

The k -cubic counterparts share the same symmetry and the constraints. Under inversion symmetry, $k_x \rightarrow -k_x, k_y \rightarrow -k_y$, while the spins do not change sign. Thus, both SOC types break inversion symmetry.

Under mirror symmetry M_x , where $k_x \rightarrow -k_x, k_y \rightarrow k_y$ and $\sigma_x \rightarrow \sigma_x, \sigma_{y,z} \rightarrow -\sigma_{y,z}$, it can be shown that h_R is invariant. In contrast, h_D is odd under M_x . The similar operation can be applied to mirror symmetry M_y . It is shown that h_R is invariant, whereas h_D is odd. The symmetry of the two common types of SOC in two-dimensional systems are summarized in Tab. III.

The mirror symmetry constraints nonvanishing components of the shift spin conductivity tensors. In this work, we consider the response to circularly polarized light normally incident on the two-dimensional plane. In this scenario, the spatial symmetry properties of the matrix element $M_{mn}^{Ic,ab}$ in the

	P	M_x	M_y	C_2
Rashba type (linear, cubic, Wurtzite)	-	+	+	+
Dresselhaus type (linear, cubic)	-	-	-	+

TABLE III. The symmetry properties of the SOC Hamiltonians under inversion (P), mirror symmetry (M_x, M_y) and rotation by π (C_2). The \pm sign denotes the evenness, oddness of the Hamiltonian under the symmetry operation.

shift spin conductivity are the same as those of the product of the spin current ($J_{mn}^{I,c}$) and the velocity operators ($v_{mn}^x v_{nm}^y$), as shown from Eq. (16). If the product is an odd function in the Brillouin zone, it leads to vanishing shift spin conductivities. h_R is M_x and M_y symmetric, such that $v_{mn}^x v_{nm}^y$ is an odd function under M_x or M_y . $J_{mn}^{I,c}$, given by the product of the spin and the velocity operator, also has to be an odd function to have nonzero responses. The mirror symmetry operation $M_d, d = x, y$, transforms the spin matrix elements $s_{mn}^I(\mathbf{k})$ to $(-1)^{\delta_{d,I}+1} s_{mn}^I(M_d \mathbf{k})$ and the velocity matrix elements $v_{mn}^c(\mathbf{k})$ to $(-1)^{\delta_{d,c}} v_{mn}^c(M_d \mathbf{k})$ [5, 7, 21]. Thus, only when the spin polarization is parallel to c , there is nonzero shift spin photocurrents. We dub this response as the longitudinal shift spin photocurrent.

h_D is even under the parity-mirror symmetry operation PM_x and PM_y , such that $v_{mn}^x v_{nm}^y$ is an odd function. $J_{mn}^{I,c}$ has to be an odd function under this parity-mirror operation to have nonzero responses. The parity-mirror operation transforms the spin matrix elements $s_{mn}^I(\mathbf{k})$ to $(-1)^{\delta_{d,I}+1} s_{mn}^I(-M_d \mathbf{k})$ and the velocity matrix elements $v_{mn}^c(\mathbf{k})$ to $(-1)^{\delta_{d,c}+1} v_{mn}^c(-M_d \mathbf{k})$ [5, 7, 21]. Thus, only when the spin polarization is perpendicular to c , there is nonzero shift spin photocurrents. We call this response as the transverse shift spin photocurrent. Furthermore, Dresselhaus SOC is $M_y M_x$ symmetric under which $v_{mn}^x v_{nm}^y$ is even and $J_{mn}^{z,x}, J_{mn}^{z,y}$ are odd. Consequently, the spin current with out-of-plane spin polarization is zero. The symmetry analysis shows that for Rashba type spin-orbit coupled systems, the nonzero components Ic of the shift spin photocurrents are xx, yy . For Dresselhaus type, the nonzero components are xy, yx .

V. ISOTROPIC ENERGY DISPERSION

For the system with isotropic energy dispersion, we mean that the band gap $d(k_x, k_y)$ has the following form

$$d = k^q \gamma, \quad (28)$$

where $q = 1, 2, 3 \dots$ and γ is only a function of spin-orbit couplings and is independent of the azimuthal angle $\phi =$

$\tan^{-1}(k_y/k_x)$. For the present cases under consideration, we have $d = \alpha_0 k$ (k -linear Rashba coupling), $d = \beta_0 k$ (k -linear Dresselhaus system), $d = \alpha k^3$ (k -cubic Rashba system), $d = \beta k^3$ (k -cubic Dresselhaus system) and $d = \alpha k + \beta k^3$ (Wurtzite system). In the presence of Zeeman coupling, the dispersion becomes

$$d = \sqrt{(k^q \gamma)^2 + \mu_z^2}. \quad (29)$$

When $\mu_z = 0$, Eq. (23) becomes

$$\text{Re}[M_{-1,1}^{Ic,xy}] = N \cdot \text{sgn}[\hat{e}_2] G \frac{\hat{d}_{\hat{e}_2}}{d} k_c \left(1 - \frac{k}{d} \frac{\partial d}{\partial k}\right). \quad (30)$$

Furthermore, we have

$$\left(1 - \frac{k}{d} \frac{\partial d}{\partial k}\right) = (1 - q), \quad \mu_z = 0. \quad (31)$$

For k -linear system $q = 1$, we always have

$$\text{Re}[M_{-1,1}^{Ic,xy}] = 0. \quad (32)$$

Namely, for k -linear system without Zeeman coupling, the shift spin photocurrent cannot be generated by the circular polarized light. For k -cubic systems, $(1 - \frac{k}{d} \frac{\partial d}{\partial k}) = (1 - 3) = -2$, it is possible to have non-zero shift spin photocurrent, but it depends on the integration of $\text{Re}[M_{-1,1}^{Ic,xy}]$, which should be confirmed by numerical calculations and symmetry constraints shown in Sec. IV.

When the Zeeman term is taken into account, the energy dispersion is $d^2 = (k^q \gamma)^2 + \mu_z^2$, and thus, in general $(1 - \frac{k}{d} \frac{\partial d}{\partial k})$ is not equal to zero even in k -linear systems. For pure k -linear Rashba system, by using Eq. (B3), we have

$$\begin{aligned} \text{Re}[M_{-1,1}^{yy,xy}] &= \text{Re}[M_{-1,1}^{xx,xy}] = N \frac{\alpha_0 \mu_z^2}{d^2}, \\ \text{Re}[M_{-1,1}^{xy,xy}] &= \text{Re}[M_{-1,1}^{yx,xy}] = 0, \\ \text{Re}[M_{-1,1}^{zx,xy}] &= -N \frac{\mu_z}{d^2} \alpha_0^2 k_y, \\ \text{Re}[M_{-1,1}^{zy,xy}] &= N \frac{\mu_z}{d^2} \alpha_0^2 k_x. \end{aligned} \quad (33)$$

Because the term N and d are independent of ϕ , we observe that after integration of ϕ , only two terms survive, which are $\sigma^{xx,xy}$ and $\sigma^{yy,xy}$. For a pure k -linear Dresselhaus system, by using Eq. (B3), we have

$$\begin{aligned} \text{Re}[M_{-1,1}^{yy,xy}] &= \text{Re}[M_{-1,1}^{xx,xy}] = 0, \\ \text{Re}[M_{-1,1}^{xy,xy}] &= \text{Re}[M_{-1,1}^{yx,xy}] = -N \frac{\beta_0 \mu_z^2}{d^2}, \\ \text{Re}[M_{-1,1}^{zx,xy}] &= -N \frac{\mu_z}{d^2} \beta_0^2 k_y, \\ \text{Re}[M_{-1,1}^{zy,xy}] &= N \frac{\mu_z}{d^2} \beta_0^2 k_x. \end{aligned} \quad (34)$$

Because the terms N and d are independent of ϕ , we observe that after integration of ϕ , only two terms survive, which are $\sigma^{xy,xy}$ and $\sigma^{yx,xy}$. These results are consistent with the symmetry consideration in Sec. IV. Furthermore, the nonvanishing shift spin conductivities are proportional to the strength

k -linear systems	d^2	xx	xy	yx	yy	zx	zy
Rashba	$\alpha_0^2 k^2 + \mu_z^2$	✓	0	0	✓	0	0
Dresselhaus	$\beta_0^2 k^2 + \mu_z^2$	0	✓	✓	0	0	0
Weyl	$\eta^2 k^2 + \mu_z^2$	0	✓	✓	0	0	0

TABLE IV. The shift spin conductivity for k -linear systems: pure Rashba (R), pure Dresselhaus (D) and Weyl systems. The nonvanishing components are labeled by ✓, whereas the vanishing components are listed as 0. Note that when the Zeeman coupling is turned off ($\mu_z = 0$), all components vanish for all systems. These results are consistent with the numerical results.

k -cubic systems	d^2	xx	xy	yx	yy	zx	zy
Rashba	$\alpha^2 k^6 + \mu_z^2$	0	0	0	0	0	0
Dresselhaus	$\beta^2 k^6 + \mu_z^2$	0	✓	✓	0	0	0
Wurtzite	$(\alpha' + \beta' k^2)^2 k^2 + \mu_z^2$	✓	0	0	✓	0	0
Rashba	$\alpha^2 k^6$	0	0	0	0	0	0
Dresselhaus	$\beta^2 k^6$	0	✓	✓	0	0	0
Wurtzite	$(\alpha' + \beta' k^2)^2 k^2$	✓	0	0	✓	0	0

TABLE V. The shift spin conductivity for k -cubic systems: pure Rashba (R), pure Dresselhaus (D), and Wurtzite (W) systems. The upper (lower) row corresponds to the pure Rashba (pure Dresselhaus) system. The nonvanishing components are labeled by ✓, whereas the vanishing components are listed as 0. These results are consistent with the numerical results.

of spin-orbit coupling. These results are listed in Table IV, where all the shift spin conductivity vanishes when $\mu_z = 0$.

The shift spin conductivities for k -cubic systems are listed in Table V, where all the non-zero components are still non-zero when $\mu_z = 0$ except for the k -cubic Rashba system. We note that in k -cubic Rashba system, all the components vanish after integration over ϕ .

It is interesting to note that the wurtzite system has dispersion similar to that of the pure k -linear Rashba system. Comparing the two systems, we have $d_x = f(k)k_y$ and $d_y = -f(k)k_x$ and $f(k) = \alpha$ for the pure k -linear Rashba system and $f(k) = \alpha' + \beta' k^2$ for the Wurtzite system. The presence of higher-order k dependence, β' , leads to the result that $\text{Re}[M_{-1,1}^{Ic,xy}]$ is proportional to β' , and in fact we have

$$\begin{aligned} \text{Re}[M_{-1,1}^{yy,xy}] &= -\frac{2Gk^2 \beta' \sin^2 \phi}{(\alpha' + \beta' k^2)^2}, \\ \text{Re}[M_{-1,1}^{xx,xy}] &= -\frac{2Gk^2 \beta' \cos^2 \phi}{(\alpha' + \beta' k^2)^2}, \\ \text{Re}[M_{-1,1}^{xy,xy}] &= \text{Re}[M_{-1,1}^{yx,xy}] = -\frac{Gk^2 \beta' \sin(2\phi)}{(\alpha' + \beta' k^2)^2}, \end{aligned} \quad (35)$$

When β' vanishes, Eq. (35) goes back to the result of the pure Rashba system. Because of the higher-order k -dependence in β' , we find that the longitudinal shift spin photocurrent survives in the absence of Zeeman coupling.

Before closing this section, we discuss the effect of the isotropic higher-order k terms, in the form of $\vec{d} = k^{q-1} \vec{d}$. The introduction of such terms does not change the symmetry of the Hamiltonian or the isotropy of the dispersion. The spin textures are not changed, either. As shown by Eq. B1, the

spin polarization is parallel to the normalized \vec{d} -vector. Notably, we find that the addition of the isotropic higher-order k terms to the k -linear Rashba and Dresselhaus systems could lead to nonzero shift spin photocurrent.

Consider the Rashba-type Hamiltonian with isotropic higher-order k . The d_x and d_y components in the Hamiltonian become

$$d_x = \alpha k^{q-1} k_y, \quad d_y = -\alpha k^{q-1} k_x, \quad (36)$$

and by using Eq. (B4), we have $G = \alpha^2 k^{2(q-1)}$. Inserting these equation into Eq. (B3), after integration of ϕ , we have

$$\begin{aligned} \text{Re}[M_{-1,1}^{xx,xy}] &= \text{Re}[M^{yy,xy}] \\ &= \frac{\alpha\pi}{d^2} k^{q-1} [\mu_z^2(q+1) - \alpha^2 k^{2q}(q-1)], \\ \text{Re}[M_{-1,1}^{xy,xy}] &= \text{Re}[M_{-1,1}^{yx,xy}] = 0. \end{aligned} \quad (37)$$

When $q = 1$ (pure Rashba), the shift spin photocurrent can be generated in the presence of Zeeman coupling. When $q \neq 1$, the shift spin photocurrent would be non-zero in the absence of Zeeman coupling. The term $q = 3$ corresponds to one part of Wurtzite system, and thus, in Wurtzite system there are non-zero shift spin photocurrent in the absence of Zeeman coupling. Furthermore, only longitudinal components (xx and yy) survive, the transverse terms (xy and yx) always vanish. We note that the above discussion does not apply to the k -cubic Rashba system with $d_x^R = \alpha k_y(3k_x^2 - k_y^2)$ and $d_y^R = \alpha k_x(3k_y^2 - k_x^2)$, because it does not relate to k -linear Rashba system by a factor of isotropic higher-order k terms. The difference between the k -linear and k -cubic Rashba Hamiltonians can be manifested in the spin textures on Fermi contours, as shown in Fig. 7 in App. C.

Consider the Dresselhaus-type Hamiltonian with higher-order k ,

$$d_x = \beta k^{q-1} k_x, \quad d_y = \pm \beta k^{q-1} k_y, \quad (38)$$

where the plus sign corresponds to the k -cubic type Dresselhaus system ($G = \beta^2 k^{2q-2}$), and the minus sign corresponds to the k -linear type Dresselhaus system ($G = -\beta^2 k^{2q-2}$). By using Eq. (B3) and after integration of ϕ , we have

$$\begin{aligned} \text{Re}[M_{-1,1}^{xx,xy}] &= \text{Re}[M^{yy,xy}] = 0, \\ \text{Re}[M_{-1,1}^{xy,xy}] &= -\text{Re}[M^{yx,xy}] \\ &= \frac{\beta\pi}{d^2} k^{q-1} [k^{2q}\beta^2(q-1) - \mu_z^2(q+1)]. \end{aligned} \quad (39)$$

Unlike the Rashba-type Hamiltonian, the Dresselhaus type Hamiltonian has the non-zero transverse components and the longitudinal components vanish. Moreover, similar to the Rashba-type Hamiltonian, the higher-order term is the key to having nonzero shift spin photocurrent in the absence of Zeeman coupling. If $q = 1$, i.e., k -linear Dresselhaus, the shift spin photocurrent always vanishes without Zeeman coupling.

VI. NON-ISOTROPIC ENERGY DISPERSION

For the system with non-isotropic energy dispersion, we mean its band gap d is written as

$$d = k^q \Gamma(\phi), \quad (40)$$

where $\Gamma(\phi)$ is a function of azimuthal angle ϕ and spin-orbit couplings. The typical systems under consideration are the k -linear Rashba-Dresselhaus system ($d = k\Gamma_2(\phi)$), k -cubic Rashba-Dresselhaus system ($d = k^3\Gamma_2(\phi)$), and the Dirac surface state with the warping term.

A. The k -linear and cubic Rashba-Dresselhaus systems

Consider the vanishing Zeeman coupling $\mu_z = 0$. It can be shown that Eq. (31) is still valid for the non-isotropic dispersion Eq. (40). Therefore, for any k -linear system of the dispersion $d = k\Gamma(\phi)$ with arbitrary function $\Gamma(\phi)$, including the k -linear Rashba-Dresselhaus system, the shift spin photocurrent always vanishes in the absence of Zeeman coupling. The details of the analytical calculation can be found in Appendix B 2 [see Eq. (B3) - Eq. (B5)]. When there is non-zero Zeeman coupling ($\mu_z \neq 0$), Eq. (23) shows that the shift spin photocurrent could be nonvanishing, as shown in Fig. 1. As shown in the figure, when $\alpha = \beta$, there is a strong response near $\hbar\omega = 0.002$ eV. When $\alpha = \beta$, the Zeeman coupling destroys the degeneracy and opens up a finite gap at $\phi = 0.25\pi, 1.25\pi$. If the chemical potential is within the gap, the joint density of states show van Hove singularities. The shift spin conductivities and the joint density of states for $\alpha = \beta$ with various Zeeman coupling are shown in Fig. 2. The shift spin conductivities (a,b) show strong peaks at $\hbar\omega = 2\mu_z$, as a result of the van Hove singularities in the joint density of states in (c). The joint density of states increase as Zeeman coupling increases; however, the shift spin conductivities do not. It suggests the dominant role of the matrix elements ($M_{mn}^{Ic;ab}$ in Eq. 8) in the shift spin conductivities.

For the k -cubic Rashba-Dresselhaus system, the longitudinal shift spin conductivities are shown in Fig. 3. Unlike the k -linear Rashba-Dresselhaus systems, the shift spin photocurrent is nonvanishing even without Zeeman coupling. Like the k -linear Rashba-Dresselhaus systems, the parameters $\alpha = \beta$ also give rise to the strongest response. When a Zeeman coupling is introduced, the shift spin conductivities exhibit peaks, as shown in Fig. 4 (a,b). Similar to the discussion in the previous paragraph for the k -linear Rashba-Dresselhaus system, the splitting of the degenerate energy bands leads to a singularity in the joint density of states, shown in Fig. 4 (c).

Furthermore, the joint density of states (JDOS) is given by $\int d^2k \delta(E_- - E_+ - \hbar\omega)/(2\pi)^2$. For the integration in \mathbf{k} , the property for the Dirac δ -function leads to $\delta(E_- - E_+ - \hbar\omega) = \frac{\delta(k-k(\omega))}{|\nabla_{\mathbf{k}}(E_- - E_+)|}$, where $k(\omega) = (E_- - E_+)/\hbar$. Thus, vanishing $|\nabla_{\mathbf{k}}(E_- - E_+)|$ leads to singularities in JDOS. We plot the maximum and minimum allowed photon energy as a function of the azimuthal angle (ϕ) in Fig. 5 and show that the van Hove singularities correspond to the region where

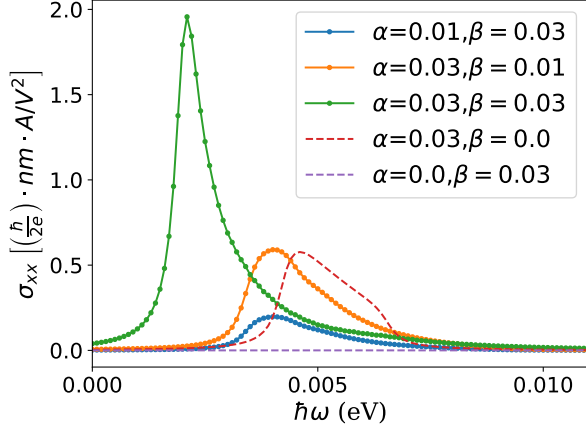


FIG. 1. The longitudinal shift spin conductivity in the k -linear Rashba-Dresselhaus system with Zeeman coupling $\mu_z = 0.001$ eV for the chemical potential at $\mu = 0.005$ eV. The effective mass of an electron is taken to be $0.05 m_0$, where m_0 is the free electron mass, in the calculation. The transverse shift spin conductivity is similar and is shown in Fig. 8 in the Appendix. Only the curves for $(\alpha, \beta) = (0.03, 0.01)$ and $(0.01, 0.03)$ are interchanged, apart from the overall sign difference.

$|\nabla_{\mathbf{k}}(E_- - E_+)|$ is minimum. There are two Fermi momenta in our two-band model, $k_f^n(\phi)$ with n defined below Eq. (5). The maximum photon energy for the direct optical transition, denoted by Ω_{max} , is given by $2d(k_f^-, \phi)$, whereas the minimum photon energy, denoted by Ω_{min} , is given by $2d(k_f^+, \phi)$. As shown in Fig. 5, for both k -linear and k -cubic Rashba-Dresselhaus systems, $\Omega_{min} = 2\mu_z$ at $\phi = 0.25\pi$ and 1.25π . As the Zeeman coupling increases, Ω_{min} become more flat; thus $|\nabla_{\mathbf{k}}(E_- - E_+)|$ decreases. This agrees with the joint density of states shown in Fig. 2 and 4 (c).

B. Dirac surface states

The surface states of three-dimensional bismuth-chalcogenides-based topological insulators can be described by the effective Hamiltonian [7, 48]

$$H_D = \epsilon_{\mathbf{k}} + \hbar v(k_x \sigma_y - k_y \sigma_x) + \lambda(k_x^3 - 3k_x k_y^2) \sigma_z, \quad (41)$$

where v denotes the Dirac velocity and the last term is the hexagonal warping term accounting for the C_{3v} lattice symmetry of the bulk Bi_2Te_3 . The warping term was observed in angle-resolved photoemission spectroscopy (ARPES) [49] and explained by symmetry arguments by [48]. The Hamiltonian preserves M_x symmetry, where M_x is the mirror reflection about the yz plane, C_3 rotation symmetry and time-reversal symmetry T . The warping term breaks M_y symmetry.

The nonvanishing components of the shift spin conductivities can be determined by the symmetry analysis, as discussed in section IV. Because of the M_x symmetry of the Hamiltonian in Eq. 41, v_{mn}^x is odd whereas v_{mn}^y is even

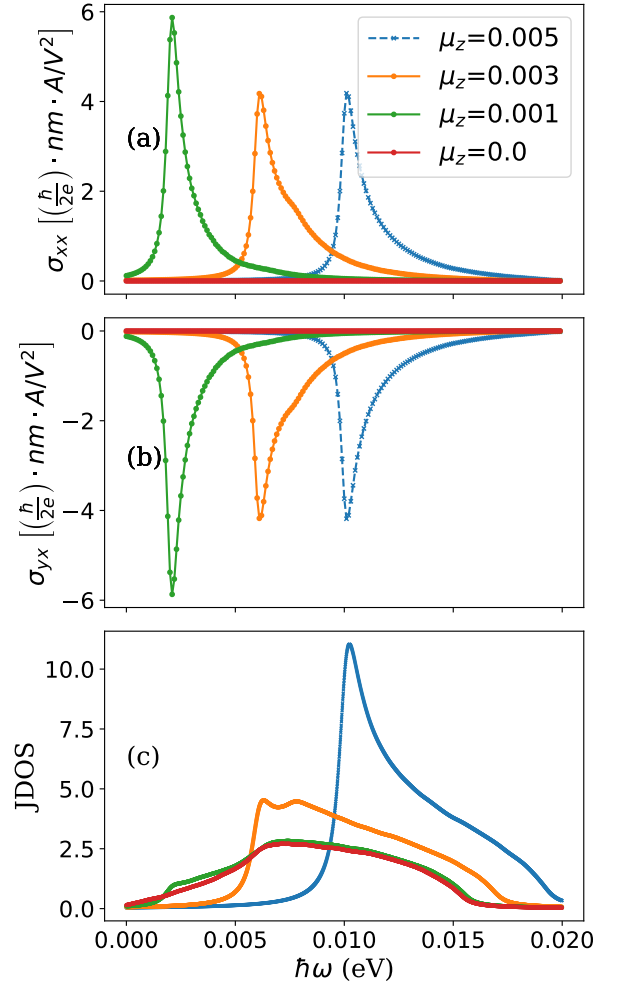


FIG. 2. The longitudinal (a) and transverse (b) shift spin conductivity and the joint density of states (c) for the k -linear Rashba-Dresselhaus system with various Zeeman coupling. $(\alpha, \beta) = (0.03, 0.03)$. The chemical potential is $\mu = 0.005$ eV, within the energy gap.

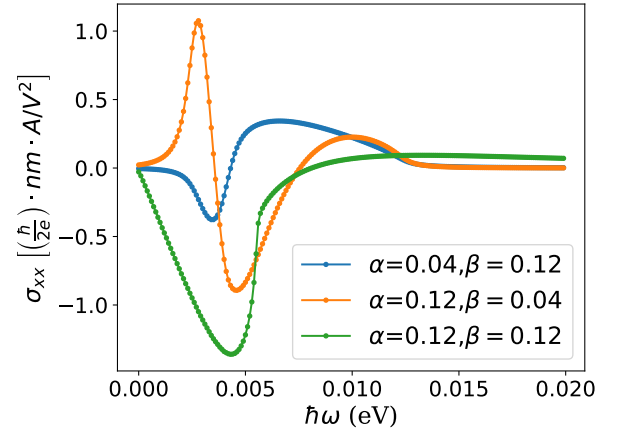


FIG. 3. The longitudinal shift spin conductivity for the k -cubic Rashba-Dresselhaus system for chemical potential fixed at $\mu = 0.01$ eV. The effective mass is set to be $0.27 m_0$ in the calculation.

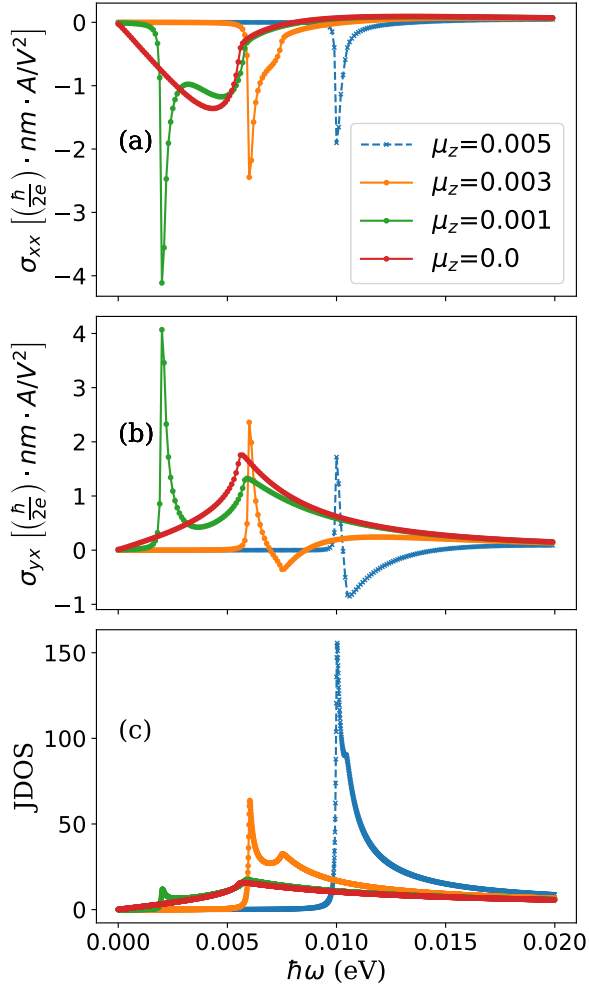


FIG. 4. The longitudinal (a) and transverse (b) shift spin conductivities and the joint density of states (c) for the k -cubic Rashba-Dresselhaus system with various Zeeman couplings. $(\alpha, \beta) = (0.12, 0.12)$. The chemical potential is $\mu = 0.01$ eV, within the energy gap.

under this symmetry operation, explicitly $v_{mn}^x(-k_x, k_y) = -v_{mn}^x(k_x, k_y)$ and $v_{mn}^y(-k_x, k_y) = v_{mn}^y(k_x, k_y)$. We consider circular polarized light incident perpendicularly to the surface; thus, $a = x, b = y$ in Eq. 8. For spin current moving in the y direction, to have a nonvanishing conductivity, the spin component has to be $I = y, z$. In contrast, for spin current moving in the x direction, the spin component for nonvanishing shift spin photocurrent is $I = x$.

The numerical results of the shift spin conductivity for the effective Hamiltonian Eq. 41 with different warping strengths are shown in Fig. 6. The shift spin conductivity grows as the warping term becomes stronger. In contrast, the joint density of states decrease mildly only at higher photon frequency. It shows that the warping term has a significant impact on the matrix element $\text{Re}[M_{nm}^{xx,xy}]$. All components have been calculated and only the significant nonvanishing component, $\sigma^{xx,xy}$, is shown. $\sigma^{zy,xy}$ is one order of magnitude smaller

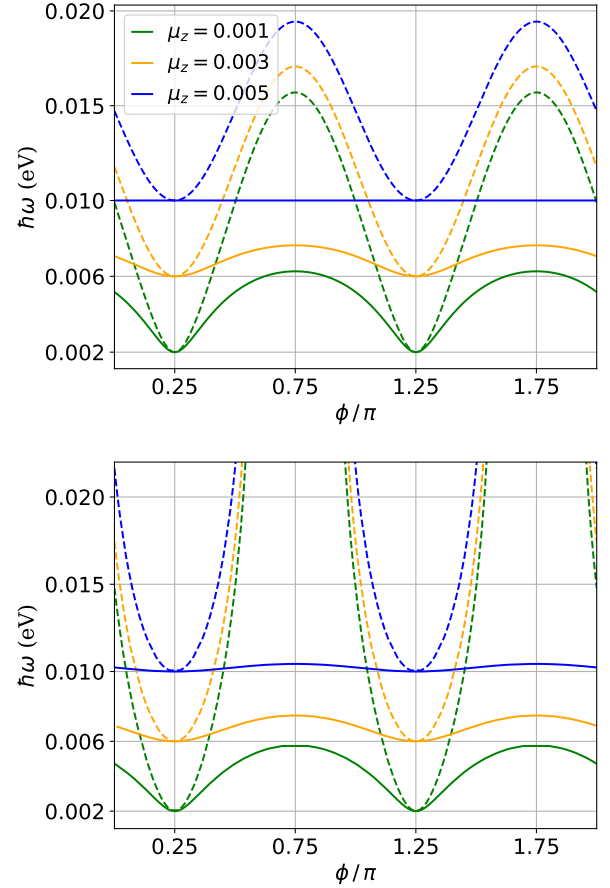


FIG. 5. The maximum (dashed lines) and minimum (solid lines) allowed photon energies for the direct transition as a function of the azimuthal angle for the k -linear (top) and k -cubic (bottom) Rashba-Dresselhaus systems with $\alpha = \beta$ and various Zeeman couplings.

and not shown. The two longitudinal circular shift spin photocurrents are equal, i.e. $\sigma^{yy,xy} = \sigma^{xx,xy}$. Thus, we only show $\sigma^{xx,xy}$.

Compared to the study of the spin photocurrent of the Dirac surface states in [19], where time-reversal symmetry is broken, in our calculation, the shift spin photocurrent is generated without breaking time-reversal symmetry and the shift charge current is zero. Nonetheless, we include the warping term, which is higher-order in k , that can lead to nonvanishing shift spin photocurrent.

VII. CONCLUSION

In this paper, we have theoretically shown that in two-dimensional systems, the shift spin photocurrent can be generated by circularly polarized light. For the k -linear Rashba-Dresselhaus systems, shift spin photocurrent always vanishes, unless a Zeeman energy is coupled in the system. For the k -cubic Rashba-Dresselhaus systems and Wurtzite systems, the shift spin photocurrents are nonzero. When Zeeman coupling

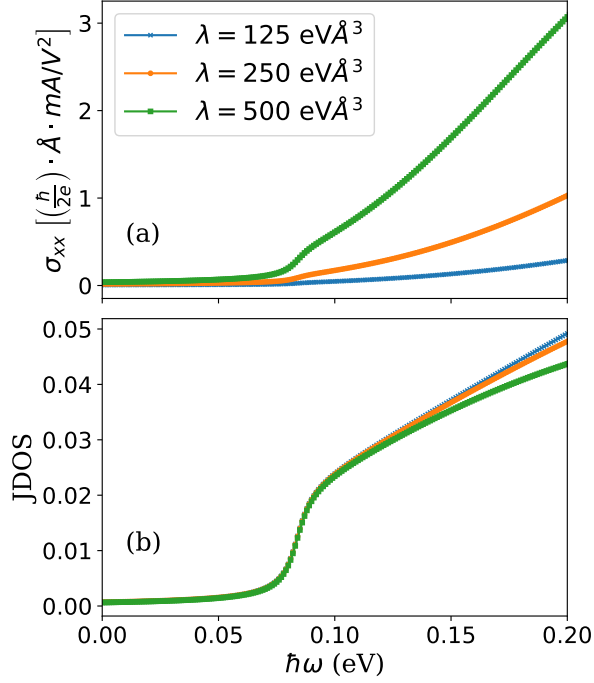


FIG. 6. The longitudinal shift spin conductivity (a) and the joint density of states (b) for Dirac surface states on topological insulators. The numerical values of the parameters for the calculations are $m = 0.13m_0$, $\hbar v = 2.5 \text{ eV}\text{\AA}$, and the chemical potential is set at 0.05 eV .

is introduced, the band-splitting leads to van Hove singularities when the states for allowed direct transitions are near the band bottom, creating peaks of the shift spin photocurrent at corresponding frequencies.

Furthermore, by symmetry analysis, we show that in Rashba type systems where mirror symmetries M_x and M_y are preserved, the spin polarization and the spin current directions are parallel. Longitudinal components of shift spin conductivities would survive, while the transverse components always vanish. In Dresselhaus type systems where the parity-mirror symmetry is preserved, the spin polarization and the spin current directions are perpendicular. In this case, transverse components of shift spin conductivities would survive, while the longitudinal components always vanish. For Dirac surface states with warping term, because of the remaining M_x symmetry, the longitudinal shift spin photocurrent is non-vanishing and increases with the strength of the warping term. The results in this work could be applied for the design of spintronic devices for spin current with particular spin polarization.

ACKNOWLEDGMENTS

H.-C. H. would like to thank Prof. Tay-Rong Chang and Dr. Yang-hao Chan for insightful discussions. H.-C. H. acknowledges the support from the National Science and Technology Council (NSTC) and the National Center for Theoretical Sci-

ences (NCTS) in Taiwan. H.-C. H. was supported by NSTC under Grant No. 113-2628-M-004-001-MY3.

Appendix A: Spin operator in k -cubic Hamiltonian

In this Appendix, we address the problems in the definition of the effective spin operator in k -cubic spin-orbit coupled systems. The Hamiltonian of the hole gas is given by the sum of both Luttinger-Kohn Hamiltonian H_{LK} [50, 51] and structure inversion asymmetric (SIA) Hamiltonian H_R and bulk inversion asymmetric (BIA) Hamiltonian H_D ,

$$H = H_{LK} + H_R + H_D + V_c(z), \quad (\text{A1})$$

where $V_c(z)$ is the confinement potential. The SIA Hamiltonian [38, 39] is given by

$$H_R = \alpha_1(\mathbf{k} \times \mathbf{J}) \cdot \hat{e}_z \quad (\text{A2})$$

and the BIA Hamiltonian [28] is given by

$$H_D = \beta_1 \mathbf{J} \cdot \boldsymbol{\Omega}, \quad (\text{A3})$$

where $\Omega_z = k_z(k_x^2 - k_y^2)$, $\Omega_x = k_x(k_y^2 - k_z^2)$ and $\Omega_y = k_y(k_z^2 - k_x^2)$.

The Hamiltonian Eq. (A1) is written in the $|J, J_z\rangle$ basis $(|3/2, 3/2\rangle, |3/2, 1/2\rangle, |3/2, -1/2\rangle, |3/2, 1/2\rangle)$, describing the light-hole ($|3/2, \pm 1/2\rangle$) band and heavy hole bands ($|3/2, \pm 3/2\rangle$). The matrix J_z in this basis is written as

$$J_z = \begin{pmatrix} 3/2 & 0 & 0 & 0 \\ 0 & 1/2 & 0 & 0 \\ 0 & 0 & -1/2 & 0 \\ 0 & 0 & 0 & -3/2 \end{pmatrix}. \quad (\text{A4})$$

The x and y components are given by

$$J_x = \begin{pmatrix} 0 & \sqrt{3}/2 & 0 & 0 \\ \sqrt{3}/2 & 0 & 1 & 0 \\ 0 & 1 & 0 & \sqrt{3}/2 \\ 0 & 0 & \sqrt{3}/2 & 0 \end{pmatrix}, \quad (\text{A5})$$

and

$$J_y = \begin{pmatrix} 0 & -i\sqrt{3}/2 & 0 & 0 \\ i\sqrt{3}/2 & 0 & -i & 0 \\ 0 & i & 0 & -i\sqrt{3}/2 \\ 0 & 0 & i\sqrt{3}/2 & 0 \end{pmatrix}. \quad (\text{A6})$$

Thus, the Hamiltonian Eq. (A1) is a 4×4 matrix. If only the heavy-hole band is concerned, we have to use the Löwdin perturbation method [15, 52] to project the Hamiltonian Eq. (A1) into a subspace spanned by $|3/2, \pm 3/2\rangle$. The resulting Hamiltonian H_{2D}^{hh} describing the heavy hole subspace is then a 2×2 matrix composed of the sum of k -cubic Rashba Hamiltonian H_R^{hh} and k -cubic Dresselhaus Hamiltonian H_D^{hh} shown in Ref. [40], where

$$H_R^{hh} = i\alpha(k_-^3\sigma_+ - k_+^3\sigma_-) \quad (\text{A7})$$

and

$$H_D^{hh} = -\beta(\sigma_+ k_+ k_-^2 + \sigma_- k_- k_+^2). \quad (\text{A8})$$

The spin-orbit parameters α and β in Eqs. (A7) and (A8) has been theoretically and experimentally studied [39, 40, 53].

The Pauli matrices in Hamiltonian H_R^{hh} and H_D^{hh} can be regarded as pseudospins. We identify the effective spin eigenstates with the $J_z = \pm 3/2$ eigenvalues, i.e. $|\uparrow\rangle = |3/2, +3/2\rangle$ and $|\downarrow\rangle = |3/2, -3/2\rangle$. We assume spin $3\hbar/2$ for the heavy holes, and thus, the effective spin operator for the hole particle should be given by

$$\mathbf{s} = \frac{3}{2}\hbar\boldsymbol{\sigma} \quad (\text{A9})$$

for three spin components and the factor of $3/2$ reflects the total angular momentum quantum numbers of the heavy holes. We stress that the overall factor $3/2$ does not affect the results if in a steady state the direction of spins is assumed to be parallel to the spin-orbit field $\mathbf{d}(\mathbf{k})/d$, as used in Ref. [54] for studying the dynamics of the direction of spins in the 2D hole system.

In this paper, we use Eq. (A9) as the effective spin operator because the effect of cubic Rashba spin splitting Eq. (A7) not only appears in 2D hole system, but also in the quasi-2D electron gas [47, 55]. Furthermore, the use of Eq. (A9) leads to the non-zero and zero shift spin currents in the k -cubic Dresselhaus and Rashba systems, respectively. The important difference between the k -cubic Rashba and Dresselhaus systems

and their interplay in the shift spin current should be determined by experiment in the future.

Appendix B: Analytical derivations

1. Matrix elements of spin

The diagonal matrix elements of Pauli matrices in the basis of Eq. (2) are given by

$$\begin{aligned} \langle n\mathbf{k}|\sigma_x|n\mathbf{k}\rangle &= -n\hat{d}_x, \\ \langle n\mathbf{k}|\sigma_y|n\mathbf{k}\rangle &= -n\hat{d}_y, \\ \langle n\mathbf{k}|\sigma_z|n\mathbf{k}\rangle &= -n\hat{d}_z, \end{aligned} \quad (\text{B1})$$

The off-diagonal matrix elements of Pauli matrices are given by

$$\begin{aligned} \langle +\mathbf{k}|\sigma_x|-\mathbf{k}\rangle &= \hat{d}_z + \frac{(-i)\hat{d}_y(\hat{d}_x + i\hat{d}_y)}{1 + \hat{d}_z}, \\ \langle +\mathbf{k}|\sigma_y|-\mathbf{k}\rangle &= i\hat{d}_z + \frac{(+i)\hat{d}_x(\hat{d}_x + i\hat{d}_y)}{1 + \hat{d}_z}, \\ \langle +\mathbf{k}|\sigma_z|-\mathbf{k}\rangle &= -(\hat{d}_x + i\hat{d}_y), \end{aligned} \quad (\text{B2})$$

where $\hat{d}_x^2 + \hat{d}_y^2 + \hat{d}_z^2 = 1$ was used. We also note that Eqs. (B1) and (B2) also satisfy the matrix elements of the commutator $[\sigma_i, H_0] = 2i\epsilon_{ijk}d_j\sigma_k$.

2. Matrix elements $M^{Ic,ab}$ for $d_z \neq 0$

Suppose that $d_z = d_z(\mathbf{k})$, we have

$$\begin{aligned} \text{Re}[M_{-1,1}^{yy,xy}] &= N \left\{ (-\hat{d}_z^2) \left[\frac{\partial d_y}{\partial k_x} \left(1 - \frac{k_y}{d} \frac{\partial d}{\partial k_y} \right) + \frac{\partial d_y}{\partial k_y} \left(\frac{k_y}{d} \frac{\partial d}{\partial k_x} \right) \right] + G \frac{\hat{d}_x}{d} k_y \left(1 - \frac{k}{d} \frac{\partial d}{\partial k} \right) \right\}, \\ \text{Re}[M_{-1,1}^{xy,xy}] &= N \left\{ (-\hat{d}_z^2) \left[\frac{\partial d_x}{\partial k_x} \left(1 - \frac{k_y}{d} \frac{\partial d}{\partial k_y} \right) + \frac{\partial d_x}{\partial k_y} \left(\frac{k_y}{d} \frac{\partial d}{\partial k_x} \right) \right] - G \frac{\hat{d}_y}{d} k_y \left(1 - \frac{k}{d} \frac{\partial d}{\partial k} \right) \right\}, \\ \text{Re}[M_{-1,1}^{xx,xy}] &= N \left\{ (+\hat{d}_z^2) \left[\frac{\partial d_x}{\partial k_y} \left(1 - \frac{k_x}{d} \frac{\partial d}{\partial k_x} \right) + \frac{\partial d_x}{\partial k_x} \left(\frac{k_x}{d} \frac{\partial d}{\partial k_y} \right) \right] - G \frac{\hat{d}_y}{d} k_x \left(1 - \frac{k}{d} \frac{\partial d}{\partial k} \right) \right\}, \\ \text{Re}[M_{-1,1}^{yx,xy}] &= N \left\{ (+\hat{d}_z^2) \left[\frac{\partial d_y}{\partial k_y} \left(1 - \frac{k_x}{d} \frac{\partial d}{\partial k_x} \right) + \frac{\partial d_y}{\partial k_x} \left(\frac{k_x}{d} \frac{\partial d}{\partial k_y} \right) \right] + G \frac{\hat{d}_x}{d} k_x \left(1 - \frac{k}{d} \frac{\partial d}{\partial k} \right) \right\}, \\ \text{Re}[M_{-1,1}^{zx,xy}] &= N \hat{d}_z \left[-\hat{d}_z \frac{k_x}{d} \left(\frac{\partial d_z}{\partial k_y} \frac{\partial d}{\partial k_x} - \frac{\partial d_z}{\partial k_x} \frac{\partial d}{\partial k_y} \right) - \frac{\partial d}{\partial k_y} + \hat{d}_z \frac{\partial d_z}{\partial k_y} \right], \\ \text{Re}[M_{-1,1}^{zy,xy}] &= N \hat{d}_z \left[\hat{d}_z \frac{k_y}{d} \left(\frac{\partial d_z}{\partial k_x} \frac{\partial d}{\partial k_y} - \frac{\partial d_z}{\partial k_y} \frac{\partial d}{\partial k_x} \right) + \frac{\partial d}{\partial k_x} - \hat{d}_z \frac{\partial d_z}{\partial k_x} \right], \end{aligned} \quad (\text{B3})$$

where the term G is defined as

$$\begin{aligned} d_x \frac{\partial d_y}{\partial k_x} - d_y \frac{\partial d_x}{\partial k_x} &= -Gk_y, \\ d_x \frac{\partial d_y}{\partial k_y} - d_y \frac{\partial d_x}{\partial k_y} &= +Gk_x, \end{aligned} \quad (\text{B4})$$

and for the systems under consideration we have

$$G = \det(\tilde{\beta}) = \beta_{xx}\beta_{yy} - \beta_{yx}\beta_{xy} \quad (\text{B5})$$

for k -linear system. By using Table I, we have $\det(\tilde{\beta}) = \alpha_0^2 - \beta_0^2$ for Rashba-Dresselhaus system, $\det(\tilde{\beta}) = \eta^2$ for Weyl

system and $G = 0$ for PST system. For k -cubic Rashba and Dresselhaus system, we have

$$G = G(k, \phi) = (3\alpha^2 + \beta^2)k^4 - 8\alpha\beta k^4 \cos \phi \sin \phi. \quad (\text{B6})$$

For Wurtzite system, it is given by

$$G = (\alpha + \beta k^2)^2. \quad (\text{B7})$$

The overall factor N is given by

$$N = \frac{\hbar}{4d^2} \frac{q\hbar^2}{2m}, \quad (\text{B8})$$

where $q = 1$ for k -linear system and $q = 3$ for k -cubic Rashba and Dresselhaus system.

Appendix C: Additional numerical results

The spin textures of the k -linear and cubic Hamiltonians are given by Eq. B1 and shown in Fig. 7.

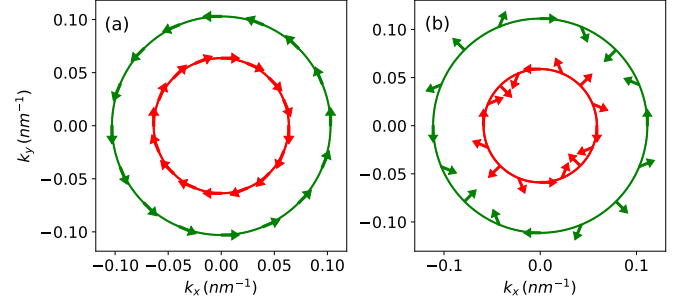


FIG. 7. The schematic of the spin textures on the Fermi contours for the k -linear Rashba (a) and the k -cubic Rashba (b) Hamiltonian.

The transverse shift spin conductivity for the linear Rashba-Dresselhaus is shown in Fig. 8.

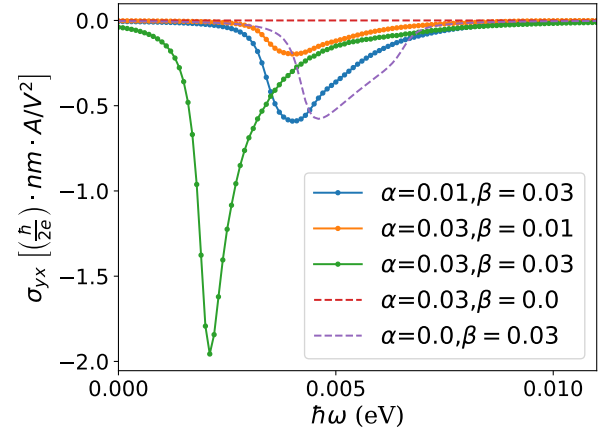


FIG. 8. The transverse shift spin conductivity for the k -linear Rashba-Dresselhaus system with out-of-plane Zeeman $\mu_z = 0.001$ eV. Compared to the longitudinal shift spin conductivity in Fig. 1, only the curves for different α, β are switched apart from the overall sign difference. The parameters for the calculation are the same as in Fig. 1.

- [1] N. Nagaosa and T. Morimoto, Concept of quantum geometry in optoelectronic processes in solids: Application to solar cells, *Advanced Materials* **29**, 1603345 (2017).
- [2] A. M. Cook, B. M. Fregoso, F. de Juan, S. Coh, and J. E. Moore, Design principles for shift current photovoltaics, *Nature Communications* **8**, 14176 (2017).
- [3] A. Pusch, U. Römer, D. Culcer, and N. J. Ekins-Daukes, Energy conversion efficiency of the bulk photovoltaic effect, *PRX Energy* **2**, 013006 (2023).
- [4] Z. Dai and A. M. Rappe, Recent progress in the theory of bulk photovoltaic effect, *Chemical Physics Reviews* **4**, 011303 (2023).
- [5] H. Xu, H. Wang, J. Zhou, and J. Li, Pure spin photocurrent in non-centrosymmetric crystals: bulk spin photovoltaic effect, *Nature Communications* **12**, 4330 (2021).
- [6] T. Morimoto and N. Nagaosa, Topological nature of nonlinear optical effects in solids, *Science Advances* **2**, 10.1126/sciadv.1501524 (2016).
- [7] J. Ahn, G.-Y. Guo, and N. Nagaosa, Low-frequency divergence and quantum geometry of the bulk photovoltaic effect in topological semimetals, *Phys. Rev. X* **10**, 041041 (2020).
- [8] J. Ahn, G.-Y. Guo, N. Nagaosa, and A. Vishwanath, Riemannian geometry of resonant optical responses, *Nature Physics* **18**, 290 (2022).
- [9] P. Törmä, Essay: Where can quantum geometry lead us?, *Phys. Rev. Lett.* **131**, 240001 (2023).
- [10] F. de Juan, A. G. Grushin, T. Morimoto, and J. E. Moore, Quantized circular photogalvanic effect in Weyl semimetals, *Nature Communications* **8**, 15995 (2017).
- [11] A. Gao, Y.-F. Liu, J.-X. Qiu, B. Ghosh, T. V. Trevisan, Y. Onishi, C. Hu, T. Qian, H.-J. Tien, S.-W. Chen, M. Huang, D. Bérubé, H. Li, C. Tzschaschel, T. Dinh, Z. Sun, S.-C. Ho, S.-W. Lien, B. Singh, K. Watanabe, T. Taniguchi, D. C. Bell, H. Lin, T.-R. Chang, C. R. Du, A. Bansil, L. Fu, N. Ni, P. P. Orth, Q. Ma, and S.-Y. Xu, Quantum metric nonlinear hall effect in a topological antiferromagnetic heterostructure, *Science* **381**, 181 (2023).

- [12] H.-C. Hsu, J.-S. You, J. Ahn, and G.-Y. Guo, Nonlinear photoconductivities and quantum geometry of chiral multifold fermions, *Phys. Rev. B* **107**, 155434 (2023).
- [13] R. W. Boyd, *Nonlinear Optics, Third Edition*, 3rd ed. (Academic Press, Inc., USA, 2008).
- [14] S. D. Ganichev and L. E. Golub, Interplay of rashba/dresselhaus spin splittings probed by photogalvanic spectroscopy—a review, *physica status solidi (b)* **251**, 1801 (2014).
- [15] R. Winkler, *Spin-orbit Coupling Effects in Two-Dimensional*

- Electron and Hole Systems*, 1st ed. (Springer Berlin, Heidelberg, Germany, 2003).
- [16] C. Aversa and J. E. Sipe, Nonlinear optical susceptibilities of semiconductors: Results with a length-gauge analysis, *Phys. Rev. B* **52**, 14636 (1995).
- [17] J. E. Sipe and A. I. Shkrebti, Second-order optical response in semiconductors, *Phys. Rev. B* **61**, 5337 (2000).
- [18] H. Xu, J. Zhou, H. Wang, and J. Li, Light-induced static magnetization: Nonlinear edelstein effect, *Phys. Rev. B* **103**, 205417 (2021).
- [19] K. W. Kim, T. Morimoto, and N. Nagaosa, Shift charge and spin photocurrents in Dirac surface states of topological insulator, *Phys. Rev. B* **95**, 035134 (2017).
- [20] T. Fujimoto, T. Kurihara, Y. Murotani, T. Tamaya, N. Kanda, C. Kim, J. Yoshinobu, H. Akiyama, T. Kato, and R. Matsunaga, Observation of terahertz spin hall conductivity spectrum in gas with optical spin injection, *Phys. Rev. Lett.* **132**, 016301 (2024).
- [21] J.-M. Lihm and C.-H. Park, Comprehensive theory of second-order spin photocurrents, *Phys. Rev. B* **105**, 045201 (2022).
- [22] R. Dong, R. Cao, D. Tan, and R. Fei, **Crystal symmetry selected pure spin photocurrent in altermagnetic insulators** (2024), arXiv:2412.09216 [cond-mat.mtrl-sci].
- [23] C. Pan, S. Hu, F. Yang, D. Yang, W. Fan, Z. Shi, L. Pan, S. Zhou, and X. Qiu, **Unveiling the nonrelativistic spin current polarization in an altermagnet** (2024), arXiv:2412.18937 [cond-mat.mes-hall].
- [24] E. I. Rashba, *Sov. Phys. Solid State* **2**, 1109 (1960).
- [25] Y. A. Bychkov and E. I. Rashba, Oscillatory effects and the magnetic susceptibility of carriers in inversion layers, *Journal of Physics C: Solid State Physics* **17**, 6039 (1984).
- [26] S. Singh and A. H. Romero, Giant tunable rashba spin splitting in a two-dimensional bisb monolayer and in bisb/aln heterostructures, *Phys. Rev. B* **95**, 165444 (2017).
- [27] K. Y. Mak, L. L. Tao, and Y. Zhou, Polarization tunable Rashba effect in 2D LiAlTe₂, *Applied Physics Letters* **118**, 062404 (2021).
- [28] G. Dresselhaus, Spin-orbit coupling effects in zinc blende structures, *Phys. Rev.* **100**, 580 (1955).
- [29] A. G. Aronov and Y. B. Lyanda-Geller, Nuclear electric resonance and orientation of carrier spins by an electric field, *Soviet Journal of Experimental and Theoretical Physics Letters* **50**, 431 (1989).
- [30] A. G. Aronov, Y. B. Lyanda-Geller, and G. E. Pikus, Spin-orbit coupling effects in zinc blende structures, *Sov. Phys. JETP* **73**, 537 (1991).
- [31] L. L. Tao, T. R. Paudel, A. A. Kovalev, and E. Y. Tsymlal, Reversible spin texture in ferroelectric HfO₂, *Phys. Rev. B* **95**, 245141 (2017).
- [32] M. Hirayama, R. Okugawa, S. Ishibashi, S. Murakami, and T. Miyake, Weyl node and spin texture in trigonal tellurium and selenium, *Phys. Rev. Lett.* **114**, 206401 (2015).
- [33] M. Sakano, M. Hirayama, T. Takahashi, S. Akebi, M. Nakayama, K. Kuroda, K. Taguchi, T. Yoshikawa, K. Miyamoto, T. Okuda, K. Ono, H. Kumigashira, T. Ideue, Y. Iwasa, N. Mitsuishi, K. Ishizaka, S. Shin, T. Miyake, S. Murakami, T. Sasagawa, and T. Kondo, Radial spin texture in elemental tellurium with chiral crystal structure, *Phys. Rev. Lett.* **124**, 136404 (2020).
- [34] L. L. Tao and E. Y. Tsymlal, Persistent spin texture enforced by symmetry, *Nature Communications* **9**, 2763 (2018).
- [35] B. A. Bernevig and S.-C. Zhang, Spin splitting and spin current in strained bulk semiconductors, *Phys. Rev. B* **72**, 115204 (2005).
- [36] Y. Kato, R. C. Myers, A. C. Gossard, and D. D. Awschalom, Coherent spin manipulation without magnetic fields in strained semiconductors, *Nature* **427**, 50 (2004).
- [37] Y. K. Kato, R. C. Myers, A. C. Gossard, and D. D. Awschalom, Current-induced spin polarization in strained semiconductors, *Phys. Rev. Lett.* **93**, 176601 (2004).
- [38] R. Winkler, Rashba spin splitting in two-dimensional electron and hole systems, *Phys. Rev. B* **62**, 4245 (2000).
- [39] R. Winkler, H. Noh, E. Tutuc, and M. Shayegan, Anomalous rashba spin splitting in two-dimensional hole systems, *Phys. Rev. B* **65**, 155303 (2002).
- [40] D. V. Bulaev and D. Loss, Spin relaxation and decoherence of holes in quantum dots, *Phys. Rev. Lett.* **95**, 076805 (2005).
- [41] A. Wong and F. Mireles, Spin hall and longitudinal conductivity of a conserved spin current in two dimensional heavy-hole gases, *Phys. Rev. B* **81**, 085304 (2010).
- [42] I. Zorkani and E. Kartheuser, Resonant magneto-optical spin transitions in zinc-blende and wurtzite semiconductors, *Phys. Rev. B* **53**, 1871 (1996).
- [43] H. J. Chang, T. W. Chen, J. W. Chen, W. C. Hong, W. C. Tsai, Y. F. Chen, and G. Y. Guo, Current and strain-induced spin polarization in InGa_N/Ga_N superlattices, *Phys. Rev. Lett.* **98**, 136403 (2007).
- [44] G. B. Ventura, D. J. Passos, J. M. B. Lopes dos Santos, J. M. Viana Parente Lopes, and N. M. R. Peres, Gauge covariances and nonlinear optical responses, *Phys. Rev. B* **96**, 035431 (2017).
- [45] J. Ibañez Azpiroz, S. S. Tsirkin, and I. Souza, Ab initio calculation of the shift photocurrent by wannier interpolation, *Phys. Rev. B* **97**, 245143 (2018).
- [46] J. Schliemann and D. Loss, Spin-Hall transport of heavy holes in iii-v semiconductor quantum wells, *Phys. Rev. B* **71**, 085308 (2005).
- [47] H. Nakamura, T. Koga, and T. Kimura, Experimental evidence of cubic Rashba effect in an inversion-symmetric oxide, *Phys. Rev. Lett.* **108**, 206601 (2012).
- [48] L. Fu, Hexagonal warping effects in the surface states of the topological insulator Bi₂Te₃, *Phys. Rev. Lett.* **103**, 266801 (2009).
- [49] Y. L. Chen, J. G. Analytis, J.-H. Chu, Z. K. Liu, S.-K. Mo, X. L. Qi, H. J. Zhang, D. H. Lu, X. Dai, Z. Fang, S. C. Zhang, I. R. Fisher, Z. Hussain, and Z.-X. Shen, Experimental realization of a three-dimensional topological insulator, Bi₂Te₃, *Science* **325**, 178 (2009).
- [50] J. M. Luttinger and W. Kohn, Motion of electrons and holes in perturbed periodic fields, *Phys. Rev.* **97**, 869 (1955).
- [51] J. M. Luttinger, Quantum theory of cyclotron resonance in semiconductors: General theory, *Phys. Rev.* **102**, 1030 (1956).
- [52] G. L. Bir and G. E. Pikus, Symmetry and strain-induced effects in semiconductors (1974).
- [53] R. Moriya, K. Sawano, Y. Hoshi, S. Masubuchi, Y. Shiraki, A. Wild, C. Neumann, G. Abstreiter, D. Bougeard, T. Koga, and T. Machida, Cubic rashba spin-orbit interaction of a two-dimensional hole gas in a strained-Ge/SiGe quantum well, *Phys. Rev. Lett.* **113**, 086601 (2014).
- [54] K. Nomura, J. Wunderlich, J. Sinova, B. Kaestner, A. H. MacDonald, and T. Jungwirth, Edge-spin accumulation in semiconductor two-dimensional hole gases, *Phys. Rev. B* **72**, 245330 (2005).
- [55] H. J. Zhao, H. Nakamura, R. Arras, C. Paillard, P. Chen, J. Gosteau, X. Li, Y. Yang, and L. Bellaiche, Purely cubic spin splittings with persistent spin textures, *Phys. Rev. Lett.* **125**, 216405 (2020).